Solar Energy
And Sustainable Development
Refereed, biannual scientific journal issued by:
The Libyan Center for Solar Energy Research and Studies

Industrial Rock Packed-Bed Heat Storage System: Thermal Behavior and Performance Assessment

Aicha Eddemani [1*], Omar Achahour [2], Hayat El Baamrani [3], Ahmed Aharoune [4], Lahcen Bouirden [5], Ahmed Ihlal [6].

[1,3,4,5]Thermodynamic and Energetics Laboratory, Faculty of Science, Ibn Zohr University, Agadir, Morocco.
[2,6]Materials and Renewable Energies Laboratory, Faculty of Science, Ibn Zohr University, Agadir, Morocco.

E-*mail:* [1] eddemani.aicha@gmail.com ,[2]omar.achahour@edu.uiz.ac.ma ,[3] hayatelbaamrani92@gmail.com , [4]aharoune@gmail.com ,[5] elahcen.bouirden@gmail.com ,[6]a.ihlal@uiz.ac.ma .

SPECIAL ISSUE ON:

The 1St International Conference on Sciences and Techniques for Renewable Energy and the Environment.
(STR2E 2025)
May 6-8, 2025 at FST-Al Hoceima-Morocco.

KEYWORDS

Rock-bed, storage material, thermal stratification, industrial packed-bed, computational fluid. dynamics (CFD) analysis.

ABSTRACT

The first industrial-scale packed-bed configuration for a Thermal Energy Storage (TES) using rocks, offering a thermal capacity of 100 MWhth, has been constructed for a Concentrated Solar Power (CSP) facility in Ait Baha, Morocco.

It employs environmentally friendly materials, using natural pebbles as the energy storage material and ambient air as the heat exchange fluid. The storage unit features an innovative design characterized by a truncated-cone form, is embedded in the ground, and operates at high temperatures ranging from 293K to 843K. To assess the thermal performance and behavior of the system, a verified Computational Fluid Dynamics (CFD) method is employed over thirty days of operation under real-world daily conditions. The results of the cyclic behavior show that the impact of thermal cycles is most pronounced in the initial cycles, while thermal stratification during both the energy storage and release phases is significantly enhanced through repeated operation. Furthermore, the system's performance improves over the thermal cycles, achieving an efficiency of 80% by the 30th cycle.

*Corresponding author.

DOI: https://doi.org/10.51646/jsesd.v14iSTR2E.800

نظام صناعي لتخزين الحرارة في الصخور بتقنية السرير المعبأ: سلوك حراري وتقييم الأداء

عائشة الدماني، عمر أشحور، حياة البعمراني، أحمد أهروان، لحسن بويردن، أحمد إهلال.

ملخص: تم إنشاء أول نظام على النطاق الصناعي لتخزين الطاقة الحرارية (TES) باستخدام الصخور، والذي يوفر سعة حرارية قدرها 100 ميغاواط ساعة حرارية، في مرفق الطاقة الشمسية المركزة (CSP) في أيت باها، المغرب. يعتمد النظام على مواد صديقة للبيئة، مثل الحصى الطبيعي كمادة للتخزين والهواء المحيط كسائل لتبادل الحرارة. يتميز التصميم بشكل مخروطي مقلوب، وهو مدفون في الأرض، ويعمل في درجات حرارة تتراوح من 293 كلفن إلى 843 كلفن. لتقييم الأداء الحراري وسلوك النظام، تم تطبيق طريقة ديناميكيات الموائع الحسابية (CFD) على مدار ثلاثين يومًا من التشغيل في ظل ظروف يومية واقعية. تظهر نتائج السلوك الدوري أن تأثير الدورات الحرارية يكون أكثر وضوحًا في الدورات الأولية، بينما يتم تعزيز التراصف الحراري بشكل كبير خلال مراحل تخزين وإطلاق الطاقة من خلال التشغيل المتكرر. علاوة على ذلك، يتحسن أداء النظام مع الدورات الحرارية، حيث يتم تحقيق كفاءة تبلغ 80 % بحلول الدورة الثلاثين.

الكلمات المفتاحية –السرير الحجري، مادة التخزين، التمايز الحراري، السرير المعبأ الصناعي، تحليل الديناميات الحركية الحسابية (CFD) .

1. INTRODUCTION

The need for energy is constantly growing due to accelerated industrialization, demographic expansion, and technological innovations [1]. Solar energy, being a clean, abundant, and renewable resource, offers considerable promise in addressing these growing energy challenges [2]. To decrease reliance on fossil fuels and significantly cutting greenhouse gas emissions, solar energy presents a viable option for meeting the world's expanding energy needs while mitigating negative environmental impacts [2]. Nevertheless, the fluctuating nature of solar energy, particularly during periods of low sunlight, presents a challenge in ensuring uninterrupted energy provision [3]. To address this limitation, the implementation of TES technologies in solar power facilities is critical for providing a consistent and reliable energy output [3, 4].

A packed-rock serves as an efficient and reliable solution for TES, positioning it as a highly appropriate choice for high-temperature TES uses in solar concentrators, particularly when air is employed as the HTF [5, 6]. These systems operate as thermocline TES systems, with rocks acting as the storage medium to capture surplus thermal energy during peak solar availability. This stored energy can be discharged during periods of low solar radiation [7]. Beyond its cost-effectiveness and favorable environmental impact thanks to the use of rocks and air, this system is also highly efficient, as it can function effectively at elevated temperatures, enhancing overall performance and scalability [7].

The thermal storage potential of rock-bed has been a central focus in numerous research studies [6, 8, 9]. Various categories of rocks have been evaluated to assess their suitability as heat storage materials, with an emphasis on their properties such as thermal capacity, conductivity, durability, and cost-effectiveness. Z. Liu et al. [10] assessed fifteen major rock types spanning igneous, sedimentary, and metamorphic classifications. Their investigation focused on examining primary thermophysical characteristics, including thermal diffusivity, heat conductivity, specific heat, and thermal expansion, as well as mechanical properties across a temperature span ranging from room temperature to 1000°C. E. Abddaim et al. [11] conducted a comparative study of four Moroccan magmatic rocks to evaluate their suitability as sustainable materials for TES. The rocks

were tested for their chemical, structural, mechanical, and thermophysical properties, with a particular focus on the impact of temperature variations and thermal cycling. The samples were subjected to five thermal cycles at 300 °C and 600 °C to evaluate changes in their structure and properties compared to the untreated samples. Parametric studies were conducted to examine the main factors influencing the performance of packed-bed heat storage configurations, including mass flow rate, fluid inlet temperature, charge-discharge cycles, and the heat absorption capability of the storage medium [3, 12, 13]. Recent reviews have highlighted the main characteristics and analytical methodologies used to examine the effectiveness of packed-bed TES systems [14-17]. These studies also summarize the major findings and outcomes from research conducted in this field. M. Tawalbeh et al. [18] have provided a detailed review of the three main energy storage methods for packed-bed systems, highlighting the recent advancements in storage materials for each approach: sensible energy, latent phase change, and thermochemical reactions. I. Calderón-Vásquez et al. [19] reviewed the heat transfer mechanisms in rock beds and examined various numerical modeling approaches. They highlighted that most existing studies focus primarily on single charge-discharge cycles, whereas a comprehensive understanding of repeated cycling operations is vital for the effective performance of these systems.
For small-scale packed-bed systems, numerous studies have been extensively documented in the literature [20-22]. However, there is a notable gap in research addressing large-scale packed bed systems, with only a few exceptions [23, 24]. This study investigates an industrial-scale packed-bed with a design capacity of 100 MWhth. The performance of the system is assessed through a time-dependent CFD simulation model, which has been effectively validated to ensure accurate and reliable simulations of its thermal dynamics and overall efficiency. Furthermore, the storage unit is assessed over 30 repeated thermal cycles, including charge, discharge, and rest phases, to investigate the influence of successive cycles on temperature layering in the packed-bed and its influence on the overall effectiveness and operational stability of the system over time.

2. METHODOLOGY

2.1. Ait Baha solar plant

The CSP plant constructed at the Ait Baha cement factory (Morocco), is designed to deliver a 3.9 MWth peak to the Organic-Rankine process for energy production. It consists of three parabolic trough collectors, each with a length of 211m (Figure 1). This thermosolar site features a packed-rock TES unit providing a capacity of 100MWth [24]. Its technology is developed by the Swiss company Airlight-Energy. The contribution of our laboratory in this project focuses on characterizing the thermal behavior and evaluating the TES unit's efficiency.

Figure 1 : Photograph of the Ait Baha CSP plant [24].

The rock used as storage material is Quartz-Sandstone. The storage unit is embedded in the ground (Figure 2) and is shaped like a truncated cone, designed to utilize lateral earth pressure for enhanced structural stability and to reduce the perpendicular stress on the walls caused by the heat-induced expansion of the rocks [25]. The lateral walls are composed of different layers

of concrete and insulating materials. The innermost layer, 0.03 m thick, is made of Ultra High Performance Concrete (UHPC), known for its outstanding mechanical strength, high thermal conductivity, and low porosity [25]. Surrounding the UHPC layer is low-density (LD) concrete, which provides structural support while maintaining low thermal conductivity. To minimize thermal losses, advanced insulation materials, including Foamglas® and Microtherm®, are integrated into the tank walls. The total thermal losses, including losses through the lateral walls, cover and bottom, remain below 3.5% of the input energy [26].

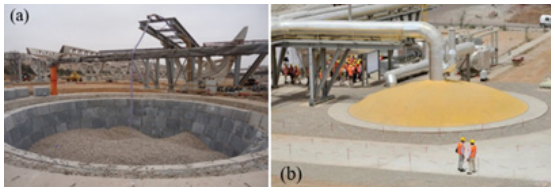

Figure 2: a) Tank filled with rocks, and b) complete system installation [24].

The system follows a daily cycle consisting of three phases: a 10h charging period, a 4h discharging phase with a high mass flow rate, and a 10h resting period to complete the cycle. The operating parameters are outlined in Table 1.

Table 1. Operating conditions of the storage unit of the Ait Baha solar power plant [24].

Parameters	
Charge inlet temperature, Tin-ch	843K
Discharge inlet temperature, Tin-disch	543K
Minimal temperature, Tmin	293K
Upper radius, Rupper	6 m
Lower radius, Rlower	5 m
Length, L	4 m
Equivalent sphere diameter, ds	0.03 m
Porosity, ε	0.35
Charging time, tcharge	10h
Discharging time, tdischarge	4h
Idle time, tidle	10h

In the charging stage, heated air is pumped into the vessel from its upper section at a temperature of 843 K and a mass flow rate of 1.716 kg/s. Conversely, during energy extraction, cold air enters the bed from the bottom at 543 K with a flow rate of 4.058 kg/s to retrieve the heat stored within the rocks.

2.2. Numerical Approach

This research employed the ANSYS-Fluent solver for numerical simulations, utilizing the finite volume method to resolve the fundamental equations governing fluid dynamics and thermal energy transfer. The storage system was modeled using a 2D-axisymmetric geometry for the computational domains. To ensure accuracy, a mesh sensitivity study was conducted to determine the optimal grid size. The computational domain was treated as a porous medium, where the rocks served as the solid component and air as the fluid component. The PISO algorithm was used for pressure-velocity correlation, and a second-order upwind scheme was implemented to solve the equations with enhanced precision. Figure 3 illustrates the numerical domain and the corresponding boundary conditions.

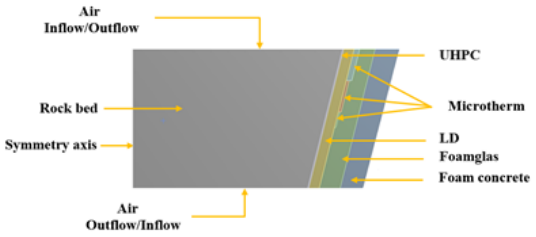

Figure 3: Overview of the numerical domain with the specified boundary conditions.

The accuracy of the numerical model was confirmed through a comparison with the experimental outcomes of A. Meier et al. [27]. The experiment involved a stainless steel cylinder, which contained rocks with an equivalent diameter of 0.02m as the thermal storage medium, through which air circulated as the HTF. The results showed a strong correlation between the experimental findings and the numerical simulations, as illustrated in Figure 4.

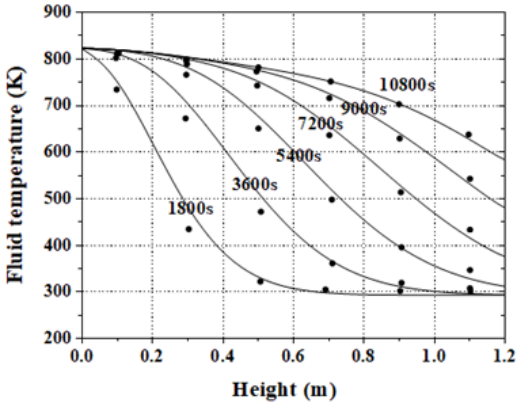

Figure 4: A comparison of the simulation predictions (line) with the experimental data (points) provided by A. Meier et al. [27].

The heat transfer model utilized in this study follows a two-phase approach adopts a two-phase approach, solving distinct energy equations for the fluid and solid phases. This method enables a more accurate representation of energy transfer between the two phases, capturing the distinct thermal behaviors of each. The fluid phase equation governs the thermal exchange within the working fluid, whereas the solid equation addresses heat conduction within the storage material. The energy conservation expressions for the air and rocks are given by Eqs. (1) and (2), respectively [28].

$$\frac{\partial}{\partial t}\left(\varepsilon\rho_f E_f\right)+\nabla\left(\vec{v}\left(\rho_f E_f+p\right)\right)=$$

$$\nabla\left[\varepsilon k_f\nabla T_f-\left(\sum_i h_i j_i\right)+\left(\overline{\overline{\tau}}\vec{v}\right)\right]+S_{heat}+h_v a\left(T_s-T_f\right) \qquad (1)$$

$$\frac{\partial}{\partial t}\left((1-\varepsilon)\rho_s E_s\right)=\nabla\left((1-\varepsilon)k_s\nabla T_s\right)+S_{heat}+h_v a\left(T_f-T_s\right) \qquad (2)$$

$\frac{\partial}{\partial t}\left(\varepsilon\rho_f E_f\right)$ and $\frac{\partial}{\partial t}\left((1-\varepsilon)\rho_s E_s\right)$ represent the rates of change of internal energy for the fluid and solid phases. ε denotes the porosity of the medium, ρ_f and ρ_s are the densities of the fluid and solid. E_f and E_s are the internal energy for the fluid and solid phases, respectively.

$\frac{\partial}{\partial t}\left((1-\varepsilon)\rho_s E_s\right)$ represents the term for convective transport of internal energy, where $\vec{v}$ is

velocity vector of the fluid, and P is the pressure of the fluid.

The terms $\nabla(\varepsilon k_f \nabla T_f)$ and $\nabla\left((1-\varepsilon)k_s \nabla T_s\right)$ represent the conductive heat flux within the fluid phase and solid phase, respectively, where k_f and k_s are the thermal conductivities of the fluid and solid, and T_f and T_s denote the temperatures of the fluid and solid.

$\nabla\left(\sum_i h_i j_i\right)$ represents the heat sources due to chemical reactions, where h_i is the enthalpy of the component, and J_i is the mass flux of the component.

$\nabla\left(\overline{\overline{\tau}}\,\vec{v}\right)$ is the viscous dissipation term, representing the conversion of mechanical energy into heat caused by fluid friction.

S_{heat} represents the external heat source term, which accounts for any thermal energy introduced into or extracted from the system.

$h_v a\left(T_f - T_s\right)$ represents the thermal interaction between the solid and fluid phases, where h_v is the heat transfer coefficient, and a is the area for heat exchange.

The numerical model is solved based on the following main assumptions: the fluid is assumed to be a perfect-gas flowing in a laminar regime, with no consideration for external heat sources, mass transfer, or chemical reactions. Additionally, the rocks are approximated as spherical to simplify the computational analysis.

The input energy during the charge represents the thermal energy provided by the HTF as it moves through the packed-bed. This energy depends on the mass flow rate of the air, temperature, and specific heat capacity, and can be mathematically expressed by Eq. (3) [29-30]:

$$E_{in} = \int_0^t \int_{T_f(0)}^{T_f(t)} \dot{m}_{ch} c_\rho \, dT_f(t) \, dt \qquad (3)$$

The energy stored throughout the storage height during the first cycle is calculated by the following equation (Eq. 4) [12]:

$$E_s = \int_0^L \rho_s c_s (1-\varepsilon)\left(T_s(y) - 293\right) dy \qquad (4)$$

Where c_s is the solid specific heat capacity, and A is the surface area.

Throughout successive cycles, the average energy stored in cycle (n) is calculated by considering the average solid temperature at the conclusion of the charge stage for cycle (n) and the temperature at the end of the idle period for cycle (n-1) (Eq. 5) [12].

$$E_{s(n)} = \rho_s c_s (1-\varepsilon) V_T \left(T_{s\_end\_ch(n)} - T_{s\_end\_idle(n-1)}\right) \qquad (5)$$

$T_{s\_end\_ch(n)}$ is the mean temperature of the solid at the conclusion of the charging period for cycle (n), and $T_{s\_end\_idle(n-1)}$ denotes the average temperature of the rocks at conclusion of the idle associated with cycle (n-1). The recovered energy E_r is defined as the heat absorbed by the air in the discharging stage (Eq. 6) [29].

$$E_r = \int_0^t \int_{T_f(0)}^{T_f(t)} \dot{m}_{disch} c_\rho dT_f(t) \, dt \qquad (6)$$

The efficiency of a thermal storage system is typically expressed as the ratio of the energy output during the discharging phase to the total energy input during the charge phase, which also accounts for the energy used in pumping during both the charging and discharging cycles.

This can be expressed mathematically as (Eq. 7) [29]:

$$\eta = \frac{E_r}{E_{in} + E_{\rho\_ch} + E_{\rho\_disch}} \qquad (7)$$

E_(p_ch) and E_(p_disch) are respectively the pumping energies during the charge and discharge processes. They are calculated using the following equation (Eq. 8) [29]:

$$E_\rho = \int_0^t \frac{\dot{m}}{\rho_f} \Delta P \, dt \qquad (8)$$

3. RESULTS

3.1. First thermal cycle

In the first phase of charging, the tank's initial temperature is set to 293 K. During this cycle, air heated by the solar concentrators is introduced into the tank at a temperature of 843 K, and a mass flow of 1.716 kg/s.

Figure (5) depicts the temperature variation within the fluid and solid phases after 3h and 10h of the initial charging process. It reveals that the thermal difference between the fluid and solid at the inlet is greater after 3h $(T_f(3h) - T_s(3h) = 135\,K)$ compared to the difference at the end of charging $(T_f(10h) - T_s(10h) = 43\,K)$. Nevertheless, the temperature of both phases remains identical across the tank. The observed results can be attributed to the heat transfer mechanisms governing the charging process. After 3h, a significant temperature difference is present, with the fluid being considerably hotter. However, as the charging process progresses, heat gradually transfers to the solid phase, reducing the temperature difference and promoting thermal equilibrium over time.

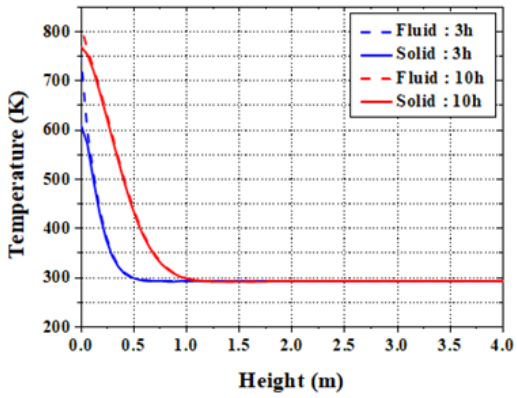

Figure 5: Temperature profiles of the solid and fluid at 3h and 10h during the initial charging.

To retrieve the stored heat during discharge, cold fluid is introduced at the bottom of the tank, having a mass flux of 4.058 kg/s and an initial temperature of 543 K. Figure (6) presents the thermal distributions in both the fluid and solid after 2h and at the completion of the first discharge process. During the first discharge, the fluid enters at a temperature higher than the one at the tank's bottom (543 K), resulting in the formation of three distinct zones within the bed: a thermocline zone located in the first quarter of the tank, followed by a thermal equilibrium zone at a temperature of 293K and a thermocline zone at the lower part of the tank.

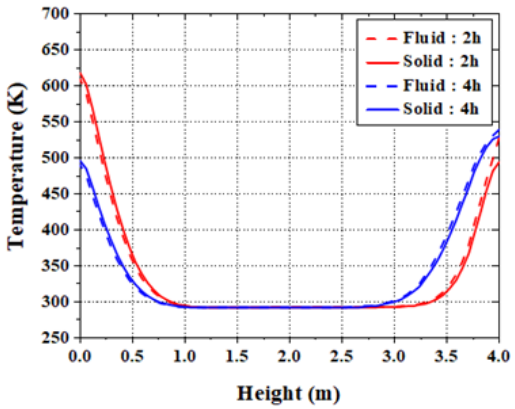

Figure 6: Temperature variations in the fluid and solid mediums after 2h and 4h of the first discharge process.

In the lower thermocline zone, the reservoir behaves as if it is experiencing the charging process because the fluid enters at a higher temperature than that obtained at the bottom. Consequently, the fluid heats the lower part of the reservoir, then a thermal equilibrium is established as it ascends, and effective discharge only occurs in the top quarter of the reservoir: the fluid temperature increases as it approaches the top of the reservoir. Therefore, in this zone, the solid temperature exceeds that of the fluid.

3.2. Cyclic operation

To characterize the storage system behavior during cyclic operation, thirty consecutive cycles are considered. Each thermal cycle consists of three phases: 10h of charging, 4h of discharging, and 10h of rest.

Figure 7 (a, b) shows respectively the temperature along the axis of the rocks medium during the first ten cycles and during the next twenty cycles. Figure (7, a) demonstrates the temperature profile during the initial charging cycle differs from the subsequent cycles; the temperature continuously decreases from the upper to the lower part of the tank during the initial charge time. However, for the second charging cycle, the temperature profile is affected by the first discharge process, which explains the appearance of two thermocline zones and a thermal equilibrium zone. Additionally, As the number of cycles increases, the two thermocline zones widen, while the thermal equilibrium zone contracts during the first three cycles.

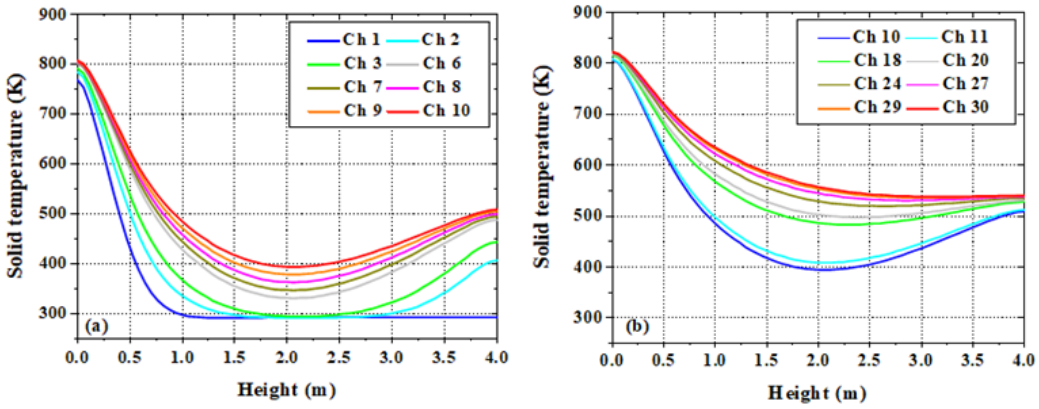

(a) (b)

Figure 7: Solid temperature distributions at the conclusion of the charging, a) for the first ten cycles, b) the subsequent twenty cycles.

Figure (7, b) illustrates the variation in solid temperature from the 10th to the 30th cycle. It can be

observed that, as the thermal cycles progress, the width of the upper thermocline zone increases at the expense of the second one, until they converge into a singular zone from the 27th cycle.
The evolution of the average solid temperature at the end of the charge period over thirty consecutive cycles is shown in Figure (8). It demonstrates that the average solid temperature grows exponentially with the progression of thermal cycles.

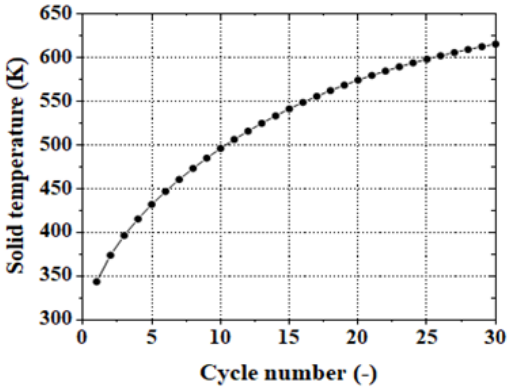

Figure 8: Evolution of the average solid temperature at the close of the charging process over thirty consecutive cycles.

The evolution of the fluid outlet temperature and the storage system's overall effectiveness throughout discharge over thirty consecutive cycles are shown in Figure (9). It indicates that the fluid outlet temperature during discharge rises significantly with the increasing cycle number, it varies between 617K in the 1st cycle and 782K in the 30th cycle. Furthermore, there is an improvement in the system efficiency as the number of cycles increases; the efficiency ranges from 3% in the 1st cycle and 80% in the 30th cycle (Figure 9).

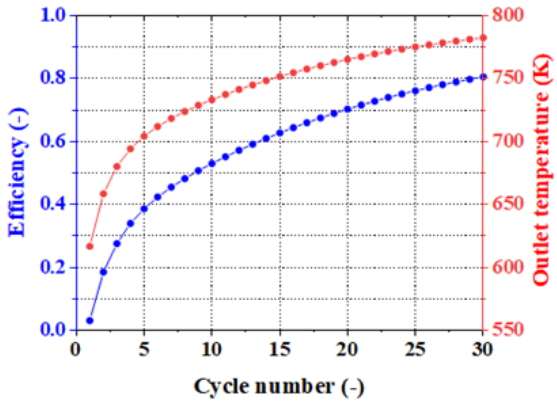

Figure 9: Progression of the outlet fluid temperature throughout discharge and the efficiency of the system over the thirty cycles.

4. CONCLUSIONS

This work presents a numerical investigation of the thermal dynamics within the energy storage system of the CSP plant in Ait Baha, Morocco. The two-phase model, which has been developed and successfully validated, is applied to analyze the storage system's response during the charge and discharge processes and to evaluate its performance. Depending on the operating conditions, numerical simulations are conducted over 30 thermal cycles, corresponding to 30 days of operation. The results of the cyclic behavior indicate that the influence of the thermal cycles is more noticeable in the initial cycles. It is found that the thermal stratification within the reservoir is enhanced with the progression of cycles. By the end of the discharge period, the fluid

outlet temperature increases from 617 K in the first cycle to 782 K in the 30th cycle. Moreover, as thermal cycles progress, the efficiency of the storage unit has been significantly improved, reaching 80% in the 30th cycle.

Authors' Contribution: Conceptualization: Aicha Eddemani, Ahmed Aharoune. Simulation and data analysis: Aicha Eddemani. Writing-Original Draft: Aicha Eddemani. Review and Editing: Omar Achahour, Hayat El Baamrani. Supervision: Ahmed Aharoune, Lahcen Bouirden. Project Coordination: Ahmed Ihlal.

Funding: This research was funded by IRESEN (Institut de Recherche en Énergie Solaire et Énergies Nouvelles, Morocco) as part of the INNOTHERM 1 project. Additional financial support was provided by the Moroccan Ministry of Higher Education and Research through the PPR/2015/31 and PPR/2015/56 projects.

Data Availability Statement: The data presented in this study are available on request from the corresponding author.

Conflicts of Interest: The authors declare no conflict of interest.

Acknowledgements: The authors express their sincere gratitude to all individuals and organizations that contributed to this work.

REFERENCES

[1] A. Z. A. Shaqsi, K. Sopian, and A. Al-Hinai, "Review of energy storage services, applications, limitations, and benefits," Energy Reports, vol. 6, pp. 288–306, Dec. 2020, doi: 10.1016/j.egyr.2020.07.028.

[2] S. Kakran, J. S. Rathore, A. Sidhu, and A. Kumar, "Solar Energy Advances and CO2 Emissions: A Comparative review of leading nations path to sustainable future," Journal of Cleaner Production, p. 143598, Oct. 2024, doi:10.1016/j.jclepro.2024.143598.

[3] A. Gil, M. Medrano, I. Martorell, A. Lázaro, P. Dolado, B. Zalba, and L.F. Cabeza, "State of the art on high temperature thermal energy storage for power generation. Part 1- Concepts, materials and modellization," Renewable and Sustainable Energy Reviews, vol. 14, no. 1, pp. 31–55, Jan. 2010, doi: 10.1016/j.rser.2009.07.035.

[4] T. Kousksou, P. Bruel, A. Jamil, T. E. Rhafiki, and Y. Zeraouli, "Energy storage: Applications and challenges," Solar Energy Materials and Solar Cells, vol. 120, pp. 59–80, Sep. 2013, doi: 10.1016/j.solmat.2013.08.015.

[5] V. Bhardwaj, S. C. Kaushik, and H. P. Garg, "Sensible thermal storage in rock beds for space conditioning: a state of the art study," International Journal of Ambient Energy, vol. 20, no. 4, pp. 211–219, 30 Mar. 2011, doi: 10.1080/01430750.1999.9675342.

[6] V. Dreißigacker, S. Zunft, Müller- H. Steinhagen, "A thermomechanical model of packed-bed storage and experimental validation". Applied Energy, vol. 111, pp. 1120–1125, 2013. doi: 10.1016/j.apenergy.2013.03.067.

[7] Z. Lai, L. Ding, H. Lyu, C. Hou, J. Chen, X. Guo, G. Han, and K. Zhang. "Experimental study on energy storage characteristics of sintered ore particle packed beds," Journal of Thermal Science, vol. 34, no. 1, pp. 242-253, Dec. 2024, doi: 10.1007/s11630-024-2079-9.

[8] N. B. Desai, M. E. Mondejar, and F. Haglind, "Techno-economic analysis of two-tank and packed-bed rock thermal energy storages for foil-based concentrating solar collector driven cogeneration plants," Renewable Energy, vol. 186, pp. 814–830, Mar. 2022, doi: 10.1016/j.renene.2022.01.043.

[9] Y. Jemmal, N. Zari, M. Asbik, and M. Maaroufi, "Experimental characterization and thermal performance comparison of six Moroccan rocks used as filler materials in a packed bed storage

system," Journal of Energy Storage, vol. 30, p. 101513, Aug. 2020, doi: 10.1016/j.est.2020.101513.

[10] Z. Liu, L. N. Y. Wong, and S.-C. Chang, "Experimental investigation of major rocks in Hong Kong as potential sensible thermal energy storage medium," Engineering Geology, vol. 343, p. 107763, Dec. 2024, doi: 10.1016/j.enggeo.2024.107763.

[11] E. Abddaim, S. Sakami, A. E. Hassnaoui, and L. Boukhattem, "Impact of temperature on chemical, thermo-physical, and mechanical properties of four rock materials for sensible thermal energy storage," Journal of Energy Storage, vol. 89, p. 111602, June 2024, doi: 10.1016/j.est.2024.111602.

[12] A. M. Rabi, J. Radulovic, and J. M. Buick, "Packed bed thermal energy storage system: Parametric study," Thermo, vol. 4, no. 3, pp. 295–314, Jul. 2024, doi: 10.3390/thermo4030016.

[13] P. Negi, Y. Singh, J. Dixit, M. Gwalwanshi, and R. Kanojia, "Experimental analysis based parametric study of packed bed heat regenerator with air as passing medium," Materials Today Proceedings, vol. 46, pp. 10488–10491, Feb. 2021, doi: 10.1016/j.matpr.2020.12.1193.

[14] G. F. Al-Sumaily, H. A. Dhahad, and M. C. Thompson, "Mixed convection phenomenon in packed beds: A comprehensive review," Thermal Science and Engineering Progress, vol. 32, p. 101242, July 2022, doi: 10.1016/j.tsep.2022.101242.

[15] W.C. Chen, Y.W. Fan, L.L. Zhang, B.C. Sun, Y. Luo, H.K. Zou, G.W. Chu, and J.F. Chen, "Computational fluid dynamic simulation of gas-liquid flow in rotating packed bed: A review," Chinese Journal of Chemical Engineering, vol. 41, pp. 85–108, Jan. 2021. doi: 10.1016/j.cjche.2021.09.024.

[16] A. Gautam and R. P. Saini, "A review on sensible heat based packed bed solar thermal energy storage system for low temperature applications," Solar Energy, vol. 207, pp. 937–956, Sept. 2020, doi: 10.1016/j.solener.2020.07.027.

[17] M. Díaz-Heras, J. F. Belmonte, and J. A. Almendros-Ibáñez, "Effective thermal conductivities in packed beds: Review of correlations and its influence on system performance," Applied Thermal Engineering, vol. 171, p. 115048, May 2020, doi: 10.1016/j.applthermaleng.2020.115048.

[18] M. Tawalbeh, H. A. Khan, A. Al-Othman, F. Almomani, and S. Ajith, "A comprehensive review on the recent advances in materials for thermal energy storage applications," International Journal of Thermofluids, vol. 18, p. 100326, May 2023, doi: 10.1016/j.ijft.2023.100326.

[19] I. Calderón-Vásquez, E. Cortés, J. García, V. Segovia, A. Caroca, C. Sarmiento, R. Barraza, and J. M. Cardemil, "Review on modeling approaches for packed-bed thermal storage systems," Renewable and Sustainable Energy Reviews, vol. 143, p. 110902, June 2021, doi: 10.1016/j.rser.2021.110902.

[20] M. M. Abera, V. R. Ancha, B. Amare, L. S. Sundar, K. V. V. C. Mouli, and S. Sangaraju, "Simulation and optimization of energy efficiency and total enthalpy analysis of sand based packed bed solar thermal energy storage," Frontiers in Heat and Mass Transfer, vol. 22, no. 4, pp. 1043–1070, Aug. 2024, doi: 10.32604/fhmt.2024.049525.

[21] R. Kothari, C. S. Hemmingsen, N. V. Voigt, A. La Seta, K. K. Nielsen, N. B. Desai, A. Vijayan, and F. Haglind, "Numerical and experimental analysis of instability in high temperature packed-bed rock thermal energy storage systems," Applied Energy, vol. 358, p. 122535, March 2024, doi: 10.1016/j.apenergy.2023.122535.

[22] H. Geng, Y. Wu, D. Ma, Y. Hao, D. Li, and H. Zhou, "Experimental study on the heat storage characteristics of rock bed heat storage system with different packing structure," Journal of Energy Storage, vol. 101, p. 113973, Nov. 2024, doi: 10.1016/j.est.2024.113973.

[23] G. Zanganeh, A. Pedretti, A. Haselbacher, and A. Steinfeld, "Design of packed bed thermal

energy storage systems for high-temperature industrial process heat," Applied Energy, vol. 137, pp. 812–822, Jan. 2015, doi: 10.1016/j.apenergy.2014.07.110.

[24] S. A. Zavattoni, G. Zanganeh, A. Pedretti, and M. C. Barbato, "Numerical analysis of the packed bed TES system integrated into the first parabolic trough CSP pilot-plant using air as heat transfer fluid," AIP Conference Proceedings, vol. 2033, p. 090027, Jan. 2018, doi: 10.1063/1.5067121.

[25] G. Zanganeh, A. Pedretti, S. Zavattoni, M. Barbato, and A. Steinfeld, "Packed-bed thermal storage for concentrated solar power – Pilot-scale demonstration and industrial-scale design," Solar Energy, vol. 86, no. 10, pp. 3084–3098, Aug. 2012, doi: 10.1016/j.solener.2012.07.019.

[26] G. Zanganeh, A. Pedretti, S. A. Zavattoni, M. C. Barbato, A. Haselbacher, and A. Steinfeld, "Design of a 100 MWhth packed-bed thermal energy storage," Energy Procedia, vol. 49, pp. 1071–1077, Jan. 2014, doi: 10.1016/j.egypro.2014.03.116.

[27] A. Meier, C. Winkler, and D. Wuillemin, "Experiment for modelling high temperature rock bed storage," Solar Energy Materials, vol. 24, no. 1–4, pp. 255–264, Dec. 1991, doi: 10.1016/0165-1633(91)90066-t.

[28] J. Ochmann, K. Rusin, S. Rulik, S. Waniczek, and L. Bartela, "Experimental and computational analysis of packed-bed thermal energy storage tank designed for adiabatic compressed air energy storage system," Applied Thermal Engineering, vol. 213, p. 118750, May 2022, doi: 10.1016/j.applthermaleng.2022.118750.

[29] M. Hänchen, S. Brückner, and A. Steinfeld, "High-temperature thermal storage using a packed bed of rocks – Heat transfer analysis and experimental validation," Applied Thermal Engineering, vol. 31, no. 10, pp. 1798–1806, July 2011, doi: 10.1016/j.applthermaleng.2010.10.034.

[30] A. Eddemani, H. El Baamrani, A. Aharoune, L. Bouirden and A. Ihlal, "Comparative Study of the Performance of Packed Beds Using Different Types of Thermal Storage Materials". Solar Energy and Sustainable Development Journal, 14 (SI_MSMS2E), 176–184, 2024, https://doi.org/10.51646/jsesd.v14iSI_MSMS2E.395.